Biomechatronic Design and Control of an Anthropomorphic Artificial Hand for Prosthetic and Robotic Applications

Loredana Zollo, Stefano Roccella, Eugenio Guglielmelli, M. Chiara Carrozza, and Paolo Dario

***Abstract*—This paper proposes a biomechatronic approach to the design of an anthropomorphic artificial hand able to mimic the natural motion of the human fingers. The hand is conceived to be applied to prosthetics as well as to humanoid and personal robotics; hence, anthropomorphism is a fundamental requirement to be addressed both in the physical aspect and in the functional behavior. In this paper, a biomechatronic approach is addressed to harmonize the mechanical design of the anthropomorphic artificial hand with the design of the hand control system. More in detail, this paper focuses on the control system of the hand and on the optimization of the hand design in order to obtain a human-like kinematics and dynamics. By evaluating the simulated hand performance, the mechanical design is iteratively refined. The mechanical structure and the ratio between number of actuators and number of degrees of freedom (DOFs) have been optimized in order to cope with the strict size and weight constraints that are typical of application of artificial hands to prosthetics and humanoid robotics. The proposed hand has a kinematic structure similar to the natural hand featuring three articulated fingers (thumb, index, and middle finger with 3 DOF for each finger and 1 DOF for the abduction/adduction of the thumb) driven by four dc motors. A special underactuated transmission has been designed that allows keeping the number of motors as low as possible while achieving a self-adaptive grasp, as a result of the passive compliance of the distal DOF of the fingers. A proper hand control scheme has been designed and implemented for the study and optimization of hand motor performance in order to achieve a human-like motor behavior. To this aim, available data on motion of the human fingers are collected from the neuroscience literature in order to derive a reference input for the control. Simulation trials and computer-aided design (CAD) mechanical tools are used to obtain a finger model including its dynamics. Also the closed-loop control system is simulated in order to study the effect of iterative mechanical redesign and to define the final set of mechanical parameters for the hand optimization. Results of the experimental tests carried out for validating the model of the robotic finger, and details on the process of integrated refinement and optimization of the mechanical structure and of the hand motor control scheme are extensively reported in the paper.**

***Index Terms*—Biomechatronic design, biorobotics, hand motor control, prosthetics.**

Manuscript received November 28, 2006; revised April 6, 2007. Recommended by Guest Editor A. Menciassi. This work was supported in part by the EU under the Neurobotics Integrated Project 2003-001917 (the fusion of neuroscience and robotics, ISTFET Project).

L. Zollo and E. Guglielmelli are with the Biomedical Robotics and EMC Laboratory, Campus Biomedico University, 00155 Rome, Italy (e-mail: l.zollo@unicampus.it; e.guglielmelli@unicampus.it).

S. Roccella and M. C. Carrozza are with the Advanced Robotics Technology and Systems Laboratory, Scuola Superiore Sant'Anna, 56025 Pontedera, Italy (e-mail: s.roccella@arts.sssup.it; carrozza@sssup.it).

P. Dario is with the Advanced Robotics Technology and Systems Laboratory and the Research Center in Microengineering, Scuola Superiore Sant'Anna, 56025 Pontedera, Italy (e-mail: dario@arts.sssup.it).

Digital Object Identifier 10.1109/TMECH.2007.901936

I. Introduction

THE HUMAN hand represents a wonderful example of a natural biomechatronic system, which still represents a benchmark for robotic designers aimed at replicating its complex functionality [1]–[3]. In the literature, several examples of robotic hands can be traced, ranging from simple grippers for industrial applications up to more sophisticated artefacts trying to mimic human mechanics [4]–[7].

Typically, end effectors of industrial robots are simple grippers or specific tools able to perform stable grasp of a limited set of known objects. They are purposively designed for a specific task, showing high dexterity in task-oriented preprogrammed applications in structured scenarios, but featuring low anthropomorphism and low manipulation capability.

Humanoid robotics is one of the fields currently devoting the most significant efforts to the design of artificial anthropomorphic hands. This is because humanoid robots are expected to achieve performance as close as possible to humans, trying to replicate them from the viewpoint of sensori-motor coordination, as well as of prompt reaction and adaptation to dynamic unstructured environments.

Prosthetics was one of the first application fields envisaged for artificial anthropomorphic hands, for obvious aesthetic as well as functional reasons. Prosthetic applications of robotic technologies impose a series of challenging requirements regarding the cosmetic appearance, the size and the weight of the hand, and its embeddable control system, which is crucial for obtaining reliable and robust hand acceptable for end users. Commercial prosthetic hands are basically simple grippers with few degrees of freedom (DOFs), a limited biomorphic appearance, and one actuator able to exert high grasping forces [8]. Consequently, the control is usually very simple but robust; a couple of commands sent by the user control gripper opening and closure. Research is addressing control algorithms [9], [10] and some of them are based on neural approaches [11], i.e., the control action is often taken as proportional to the superficial electro myographic (EMG) signals extracted by surface electrodes applied to a couple of antagonistic user's residual muscles. The control of the Ottobock prosthesis is paradigmatic for a typical prosthetic control [11]. In [10] and [12], a hybrid control is presented, where a digital controller operated by means of myoelectric signals converts the user's grasping intention (as specified by the EMG signal) into an order for the control of the prosthesis. In it, sensors to the prosthesis and feedback to the user have been added [10], [13]. Anyhow, present commercial prosthetic hands still have a series of limitations [35] related

to the reduced functionality and sensitivity with respect to the human hand. The availability of bidirectional neural interfaces, with the peripheral or central nervous system (PNS or CNS), and of light and powerful actuators are the two main key-enabling technologies still missing to produce a real breakthrough in this field of robotics.

The main goal of this paper is to present an integrated design approach between mechanics and control [14] applied to an underactuated anthropomorphic artificial hand for robotic and prosthetic applications.

This means that the overall hand design is the result of a full integration of mechanics and control, where the hand dynamic modelization and the design and development of the control system contribute to the refinement and optimization process of the hand mechanical parameters. This approach has been successfully applied to the design of mechatronic technologies outside the biomedical area [45], [46].

The core of the hand mechanics is the underactuated cable mechanism used for each finger. The hand is able to adapt itself to the object shape without requiring complex control techniques. Only one actuator moves the three phalanges of each finger, so that their motion is coupled. This mechanism is suitable for both prosthetic and robotic applications whenever the versatility of the grasp, the weight and the dimensions requirements are critical design challenges. The proposed artificial hand implements the "soft gripper" mechanism proposed by Hirose [36] based on embedding torsion springs in each finger joint. This same mechanism has also been deeply studied by Kaneko *et al*. [39], [40] for fast grippers. In this paper, we propose to focus on the early-stage integration between control and mechanics (mechatronic design) so as to choose the mechanical parameters in order to optimize the tracking of a reference trajectory in the joint space for all the fingers.

To improve the anthropomorphic behavior of the biomechatronic hand, a bio-inspired approach is also followed in designing the artificial hand motor control. The control system of a robotic device can be biologically inspired at different levels. It can be conceived in order to replicate in the robotic system a motion that is human-like, for example in preshaping, grasping, or manipulation [15], [16]. On the other hand, studies on force regulation and stability grasp in humans can be resumed to pursue a natural stability and force control in grasping and manipulation [17]–[19]. To this regard, many approaches to control can be referred, based on direct or indirect force control, such as compliance control [20]–[25], impedance control [26]–[31], or hybrid position/force control [33].

The ultimate goal of the biomechatronic design of the hand as presented in this paper is to replicate natural finger motion as a result of an optimization of the control scheme as well as of the kinematics and the dynamics of the proposed artificial hand.

To this purpose, the authors exploited data on human behavior during fingers motion, with particular attention to fingertip and joint trajectories, during closing the hand fingers towards palmar grasping of a cylindrical object (i.e., preshaping) [15], [16]; these data have been used as reference for the control system. Design goal of the control system is addressed to obtain a good trade-off between simplicity and functionality, by optimizing proportional–derivative (PD) control with gravity compensation [33], [34], taking into account the constraints of the underactuated mechanism. Two different versions of the control system have been developed and compared, one in the joint space and the second in the slider space, where the slider is the mechanism for producing tension in the cable transmission. Further, the control in the slider space was also used to provide data for optimising mechanical design and obtain the set of parameters that allow the best mimicking of the reference trajectories reported from the observation of natural human fingers.

This paper is organized as follows. Section II describes the biomechatronic hand design and the main features of the first prototype. System model development and theoretical formulation of two artificial hand control laws are presented in Section III. Simulation tests on the comparison between the two proposed control laws in the case of one finger motion while closing in absence of gravity and the optimization process of the hand design are reported in Section IV. Modeling, simulation tests and design refinement have been carried out by means of the joint use of computer-aided design (CAD) tools (i.e., Pro-Engineer) and simulation software (i.e., MATLAB/Simulink), and results related to the two control systems are based on the assumption of 2-D finger motion representing the preshaping phase of a cylindrical object. Finally, Section IV also presents and discusses results of the experimental validation of the simulated closed-loop control system carried out on the first hand prototype.

II. Design of the Hand Prototype

A. Biomechatronic Design Approach

The human hand is a complex system hard to replicate in its performance and features. The biomechatronic design approach consists of developing an artificial hand that replicates the human hand in its fundamental structure (weight, dimensions, minimum number of fingers, essential DOF of the fingers, essential finger kinematics, etc.), reproducing essential functions of it (stability and adaptability of the grasp, human like finger motion, etc.). In order to develop a reliable system satisfying fundamental functional requirements, the mechanical and control solutions must be simple. The design approach is composed of different phases. The first stage of the work is the analysis of the morphological and functional characteristics of the human hand. In particular, requirements for the design and development of the artificial hand are extracted from the study of the human hand [1] from the viewpoint of anatomy, gesture and grasping capabilities, and kinematic and dynamic performance.

Basic capabilities of the human hand can be summarized as follows:

- reaching and preshaping;
- grasping;
- manipulation with stable grasp;
- exploration with sensori-motor coordination;
- gesture expressiveness.

The actuation finger mechanism, as well as the type of proprioceptive and exteroceptive sensors to be embedded in the mechanical structure have been selected in order to obtain a high

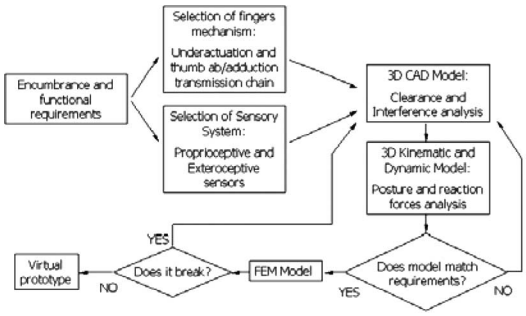

Fig. 1. Mechanical design flow of the underactuated artificial hand.

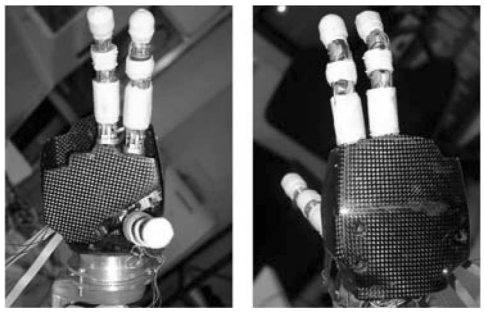

Fig. 2. Three-fingered artificial hand.

Fig. 3. Artificial finger mechanical structure that mimics the human finger.

degree of anthropomorphism of the robotic artifact; some level of customization of the hardware components to the specific requirements of the two addressed application fields (humanoid robotics or prosthetics) has been also taken into account.

As a second design stage, a virtual hand prototype has been built using CAD tools. This simulation allows studying the robotic hand kinematics and dynamics, and verifying the design against the functional requirements. Interaction forces among the components are estimated. These forces are used as input data to the structural analysis, and if one component is not able to sustain the nominal external loads, the hand is redesigned. Mechanical features of each component are then iteratively modified and verified by using the virtual prototype.

In this way, the design process is iterated in order to optimize the robotic hand. The final virtual prototype will satisfy the initial requirements; and its kinematics, dynamics, and structural characteristics are eventually fixed. The mechanical design flow, as shown in Fig. 1, ends with the production of the technical drawings of each mechanical component of the hand system.

The overall hand design process, then, proceeds with the dynamic modeling and the formulation and development of the control law adapted to the conceived mechanics. Thus, mechanics and control are merged in a unique closed-loop system in order to study the performance of the integrated system, and optimize the hand design by carrying out a comparative analysis with the human hand behavior.

B. Underactuated Artificial Hand

The artificial hand reproduces the human one in its fundamental structure. The weight, the dimensions, and the inertia of the fingers are similar. The finger kinematics, including the possibility of the thumb to change the flexion plane (adduction/abduction), are approximated using simple mechanisms (pin joints and worm/worm wheel transmissions). This approximation can be considered quite good for the proximal and distal joints. Human metacarpal joints are more complex because their axis of rotation changes during the motion due to the surface profile of the joint. This allows the finger to adduct and abduct while it flexes, becoming stiffer. This feature is not replicated in the artificial hand because the fingers are placed in the palm in a position that statistically allows grasping different objects currently used by patients or humanoid robots. The human hand can be considered underactuated because the *flexor digitorum profundus* tendon runs across all the finger joints, and is attached to the distal phalange [1].

Several underactuated hands have been developed recently [42], [43]. In this paper, the mechanics is conceived to reduce the hand weight keeping acceptable performance in terms of grasp stability and dexterity (especially for the opposition capabilities of the thumb).

The artificial hand (in Fig. 2) is composed of three underactuated fingers (index, middle, and thumb), which are actuated by three dc motors placed in the lower part of the forearm (e.g., the socket for an upper prosthetic limb or the robotic arm for a robotic artefact), reproducing the role of natural extrinsic muscles. The hand prototype is an evolution of the RTR II prosthetic hand presented in [35], especially for the selected ratio between the number of actuators and the number of DOF, and for the adopted solution for underactuation of the fingers.

Three can be considered the minimum number of actuated fingers in order to have a stable grasp, while minimizing the hand weight. Each finger is composed of three phalanges in order to have an anthropomorphic self-adaptive stable grasp augmenting the number of contact points on the object. To satisfy the aesthetic requirements, the hand can be covered with a silicone glove that includes two additional passive fingers (ring and little).

Each finger can flex as a result of the cable, which runs along its volar side and wraps around idle pulleys placed in each joint according to the soft gripper mechanism [36]. The extension of the finger is obtained by means of torsion springs placed at each joints. In this way, the number of motors is reduced, and the actuation system is lighter.

The artificial hand finger dimensions are very close to the human finger, and have been taken from the GeBOD (generator of body data) [41] anthropometric database, based on a standard 95th percentile human male subject (Fig. 3).

The hand is able to adapt itself to the object shape due to the cable finger mechanism [37].

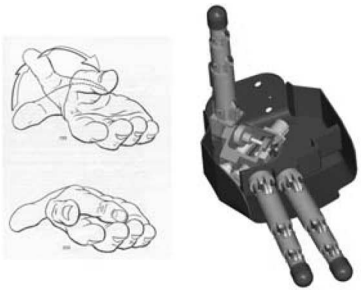

Fig. 4. Abduction and the adduction of the human thumb and the 3-D CAD model of the artificial thumb mechanism.

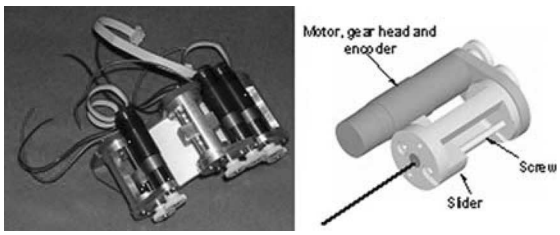

Fig. 5. Actuators carrier mimicking the natural extrinsic muscles and the 3-D CAD model of the actuation and transmission system of one finger.

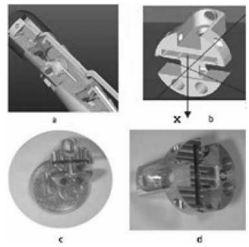

Fig. 6. Three-component force sensor.

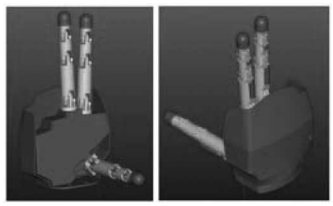

Fig. 7. 3D CAD model of the artificial hand.

The thumb can abduct and adduct by moving from the palmar position to the lateral position and vice versa, as depicted in Fig. 4. The dc motor (1016 006C FAULHABER with IE2-512 encoder and 64:1 gearbox) used to generate the abduction/adduction motion is placed inside the palm, and can rotate the thumb through a worm wheel gear mechanism. It is not a backdrivable device, so the thumb can fix its position when the power is off.

The artificial hand has 10 DOF and 4 degrees of motion (DoM): 1 DoM/3 DOF for each finger (flexion/extension) and 1 DoM/1 DOF for thumb opposition (adduction/abduction).

The palm is composed of three components, namely the outside shell, the inside frame, and the inside shell, all made of carbon fiber. This material conveys high strength and light weight to the structure. The fingers are made of aluminium alloy (2011 aluminum Speedal); they have a cylindrical shape in order to optimize the grasp and the contact area with the object.

The main artificial hand's measured features are as follow:

- weight: 250 gm (palm, three fingers, abduction/adduction thumb mechanism with its dc motor) + 70 gm (optional extra two fingers);
- dimensions: 191 mm × 95 mm × 40 mm (length × width × thickness);
- maximum cylindrical grasping force: 35 N;
- maximum tip-to-tip grasping force: 15 N;
- maximum closing time: 6 s;
- thumb joint abduction/adduction range: 0°–120°;
- finger joint flexion range: 0°–90°.

Each finger is actuated by one dc motor (1727 006C FAULHABER with IE2-512 encoder and 16/7 14:1 gearbox) located in the forearm, which pulls a cable through a linear slider connected to the motor through a leadscrew (Fig. 5). This forearm module, which also integrates all the electronics for controlling and driving the device has an estimated total weight of about 600 gm. It is worth noticing that the overall weight of the hand plus forearm modules is below 1000 gm, which is an acceptable value for both prosthetic and robotic applications.

The artificial hand is equipped with four incremental encoders (one for each motor), two three-component force sensors (one at the thumb and the other at the index fingertip) (Fig. 6) and eight Hall effect switches (two on each slider and two on the thumb abduction/adduction mechanism) for the encoder calibration.

C. 3D CAD Model and Dynamic Analysis

The 3D CAD model of the artificial hand was built by using ProEngineer (Fig. 7). Clearance and interference problems were virtually analyzed through a dedicated feature of this software tool.

The kinematics and dynamics of the artificial hand have been simulated by using ADAMS. This software is a multibody analysis simulation program that solves the rigid body dynamic equilibrium equations and directly interfaces with ProEngineer. For the first prototype, the starting values of the design parameters were determined by building the virtual prototype, and analyzing it through these simulation tools. The mechanical structure of the force sensors and of the hand were designed and verified by means of finite element method (FEM) simulations implemented on ANSYS.

The dynamic behavior of the underactuated finger during object reaching and grasping is mainly influenced by three design parameters: 1) the pulley radius; 2) the torsion spring stiffness; and 3) the torsion spring preload.

The value of these parameters depends on the different hand functionality to be considered. For instance, the first prototype of the hand was developed focusing on the grasping phase, i.e., it was aimed at achieving a stable grasp without slippage on the object surface and with a uniform grasping force. In this case, from 3D CAD simulations, the set of parameters resulted in

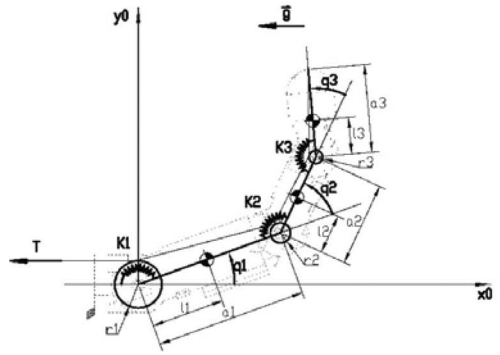

Fig. 8. Finger scheme: a_1, a_2, and a_3 are the three link lengths representing the three finger phalanges; $r_1 r_2$, and r_3 are the pulley radii; K_1, K_2, and K_3 are the stiffness coefficients of the torsional springs at each joint; and T is the tension of the cable wrapping around each pulleys.

the following values (see also Fig. 8):

- $r_1 = 7 \times 10^{-3}\, m\, r_2 = 3 \times 10^{-3}$ m, $r_3 = 2 \times 10^{-3}$ m for the pulley radii;
- $K_1 = 10.93 \times 10^{-3}$ N·m/rad, $K_2 = 6.69 \times 10^{-3}$ N·m/rad, $K_3 = 5.03 \times 10^{-3}$ N·m/rad for spring stiffness coefficients;
- $q_{01} = -1.57$ rad, $q_{02} = -1.21$ rad, $q_{03} = -1.19$ rad for the equilibrium joint configuration imposed by the spring preload.

The springs are commercial components, and their stiffness has been choosen from catalog in order to be close to the values calculated in the simulations. As described later, the spring preload is essential in determining the dynamic behavior of the finger, so that the little differences between the optimally calculated values and the commercial ones can be compensated by tuning the spring preload.

This paper is mainly concerned with the analysis of the dynamic behavior of this first prototype focusing on the problem of controlling the hand closure as a first design goal. More specifically, the analysis to be performed shall allow assessing whether design parameters are optimized for the finger motion during closing in free space, without interaction with the environment. To this aim, a control law for one underactuated finger is formulated and a parametric simulation tool is developed. It is worth mentioning here that this is a significant advancement with respect to the commercial simulation tools that typically could allow neither modeling of underactuated finger (with coupled joints and cable wrapping around the pulley) together with the control scheme nor on-the-fly changes of design parameters while tracing back all mechanical modifications to the 3-D CAD model.

III. Control System

The control is aimed at exploiting the main properties of underactuation (i.e., the self-adaptation and the reduced number of DoMs) to perform motion tasks in a way comparable to the human case. Basically, this paper takes into account the control and redesign of only one finger (Fig. 8), but the results obtained can be easily extended to the other two fingers that feature a very similar mechanical structure.

The ordinary task considered for the design and development of the motion control law is the finger preshaping for a palmar grasp of a cylindrical object.

As shown in Fig. 5, the actuation system for each three-phalanx finger is based on one dc motor moving a slider mechanism, which transmits motion to the phalanges. In particular, the three joints corresponding to the three phalanges are coupled in terms of kinematics and dynamics.

Kinematic coupling among the joints is related to the slider kinematics by the relation

$$x_S = r_1 (q_1 - q_{10}) + r_2 (q_2 - q_{20}) + r_3 (q_3 - q_{30})$$
$$\ddot{x}_S = r_1 \ddot{q}_1 + r_2 \ddot{q}_2 + r_3 \ddot{q}_3 \quad (1)$$

where

- $q = [q_1, q_2, q_3]$ and $\ddot{q}$ are the vectors of the joint angles and accelerations, respectively;
- r_1, r_2, and r_3 are the pulley radii;
- x_S and $\ddot{x}_S$ are the slider displacement from the static equilibrium configuration and acceleration, respectively;
- q_{10}, q_{20}, and q_{30} are the initial equilibrium joint angles.

The dynamic relation among the joints is expressed in terms of joint torques τ_1, τ_2, and τ_3 and cable tension T as

$$\tau_1 = r_1 T$$
$$\tau_2 = r_2 T$$
$$\tau_3 = r_3 T. \quad (2)$$

From (1) and (2), it is conceivable to control the artificial hand either in the joint space or in the slider space, as formulated in the following. Joint space stands for the space where the joint variables of position, velocity, and acceleration are defined; on the other hand, the slider space is the space where the slider variables of position, velocity, and acceleration are defined. In other words, the slider motion corresponds to the motion of the free end of the cable when the joints move from the initial to the final equilibrium configuration.

A. PD Control in the Joint Space With Elastic Compensation

Dynamic relation (2) is used to actively control the first joint (i.e., q_1) and passively move the joints q_2 and q_3. The proposed control law is a modified version of the standard PD control in the joint space with gravity compensation [38] and is expressed as

$$\tau = K_P \tilde{q} - K_D \dot{q} + g(q) + \tau_e \quad (3)$$

where $\tilde{q} = q_D - q$ is the joint position error defined as the difference between the reference set point (q_D) and the current joint angle q, $g(q)$ is the estimation of the joint gravitational torque, and K_P and K_D are the diagonal gain matrices for the proportional and derivative control actions, respectively. In addition to the standard PD control plus gravity compensation, an elastic term is introduced (i.e., τ_e), in order to compensate for the preloaded springs located at each joint (Fig. 8).

The joint elastic torque is expressed as

$$\tau_e = K_e (q - q_0)$$

where K_e is the diagonal matrix of the spring stiffness coefficients and q_0 is the vector of the joint angles, which when multiplied for K_e, provides the torsional spring preload.

In the specific case of a single underactuated three-phalanx finger, (3) is referred only to the first joint, and K_P, K_D, and K_e are positive scalars.

Note that the PD control in the joint space in (3), generates only the torque command for the first joint, which needs to be converted in cable tension through (2) to control the finger.

B. PD Control in the Slider Space with Elastic Compensation

Control in the slider space exploits (1) to move joints q_1, q_2, and q_3 by directly controlling the slider motion. Hence, a PD control with elastic compensation is formulated in order to provide the cable tension needed to move the slider as desired. The resulting control law is

$$T_S = K_{PS}\tilde{x}_S - K_{DS}\dot{x}_S + g_S(q) + T_{e\_S} \tag{4}$$

where

- $\tilde{x}_S = x_D - x$ is the slider position error defined as the difference between the reference set point (x_D) and the current slider position x;
- $K_{PS}\tilde{x}_S$ and $K_{PS}\dot{x}_S$ are the proportional and derivative actions on the slider position and velocity, respectively;
- $g_S(q)$ is the effect of the gravitational torque at the level of slider;
- T_{e_S} is the elastic contribution of the preloaded springs.

Mechanical relations (1) and (2) allow moving from the joint space to the slider space, and vice versa.

It is worth noticing that the PD control in the slider space has an advantage over the PD control in the joint space—of directly generating the cable tension needed to move the finger, and which is uniquely related to joint torques through (2). It accounts for the kinematic and dynamic relations between slider and joints by means of (1) and (2).

IV. Validation and Optimization of the Hand Design

Simulation tests have been carried out in order to achieve the following goals.

- *Goal 1:* to implement the two proposed control laws and compare their performance;
- *Goal 2:* to experimentally validate the simulated model and the control law by replicating simulation tests on the real robotic finger;
- *Goal 3:* to model the motion of the human finger, and compare the behavior of the biomechatronic hand with the human hand; and
- *Goal 4:* to iteratively refine the mechanical design in order to best fit the human behavior.

Basically, *Goals 1* and *2* are preliminary steps to analyze the control performance, to choose the control law to be implemented on the real artefact, and to verify the reliability of the simulated model. As a further step, the hand optimization can follow by progressively redesigning and evaluating the closed-loop system integrating mechanics and control.

A. Simulation and Preliminary Experimental Validation of the Closed-Loop System

In order to achieve *Goals 1* and *2*, each finger has been regarded as a three-joint planar manipulator whose dynamics is expressed as

$$B(q)\ddot{q} + C(q,\dot{q})\dot{q} + g(q) + K_e(q - q_0) = \tau \tag{5}$$

and the underactuation system is described by (1) and (2), under three hypotheses: 1) the cable is inextensible, and its mass is negligible; 2) friction is negligible; and 3) the cable flexes the finger while the torsion springs placed at each joint extend it.

In (5),

- $B(q)$ is the (3×3) joint inertia matrix;
- q, $\dot{q}$, and $\ddot{q}$ are the (3×1) joint position, velocity, and acceleration vectors, respectively;
- $C(q,\dot{q})\dot{q}$ is the (3×1) vector of centrifugal and Coriolis torques;
- $K_e(q - q_0)$ is the (3×1) elastic torque vector;
- $g(q) = 0$ because gravity vector is perpendicular to motion plane (2-D motion hypothesis).

A simulated environment has been developed in MATLAB/Simulink in order to model the finger mechanics and dynamics, and implement control laws (3) and (4). In particular, when a control in the joint space has been tested, a cubic polynomial trajectory in a time interval of 6 s has been considered for joint q_1, having $q_{i1} = 0$ rad as initial configuration and $q_{f1} = 1.50$ rad as final configuration. This range of variation corresponds to the set of reachable configurations for the first finger joint of the realized prototype while closing.

On the other hand, when control law (4) is implemented, a reference trajectory for the slider is provided to the control. It corresponds to a cubic polynomial trajectory from the initial slider position of 0 m up to the final position $x_{\text{slider}} = 0.0163$ m (i.e., the slider displacement, which allows reaching a joint position of $q_1 = 1.50$ rad).

In order to develop the model of the robotic finger and to test the two control laws, the first set of mechanical parameters of the prototype has been used. In particular,

- $q_1 \in [0, 1.50]$ rad is the range of variation of the first joint;
- $K_e = \text{diag}(10.93,\ 6.69,\ 5.03)10^{-3}$ N·m/rad is the diagonal matrix of the spring stiffness coefficients;
- $r_1 = 7 \times 10^{-3}$ m, $r_2 = 3 \times 10^{-3}$ m, $r_3 = 2 \times 10^{-3}$m are the values of the pulley radii;
- $q_0 = [-\pi/2 - 1.21 - 0.95]^T$ rad is the equilibrium joint configuration, which multiplied for K_e provides the torsional spring preload;
- $T_0 = 2.45$ N is the initial value of the cable tension.

The different K parameters in the two control laws have been set empirically by pursuing maximum performance within the stability limits. The control gains have been set to $K_P = 0.02$ and $K_D = 6 \times 10^{-7}$ for the PD control in the joint space with elastic compensation, and $K_{PS} = 4500$ and $K_{DS} = 80$ for the PD control in the slider space with elastic compensation.

Simulation results for the two control laws during the task of closing the finger in the x–y plane are reported in Figs. 9 and 10.

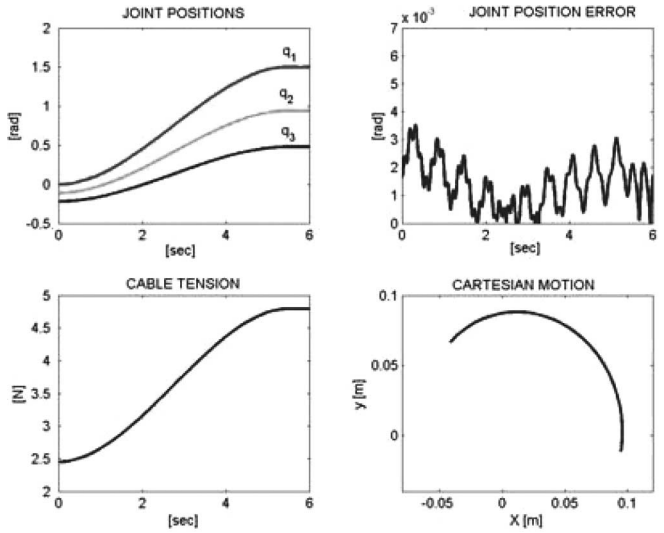

Fig. 9. Simulation results for the control in the joint space: (a) finger joint trajectories; (b) joint position error; (c) cable tension related to joint torque through (2); and (d) tip motion in the Cartesian space.

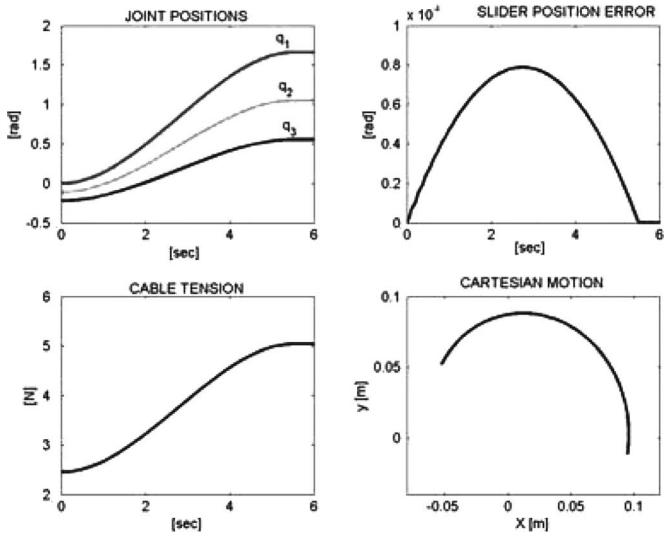

Fig. 10. Simulation results for the control in the slider space: (a) finger joint trajectories; (b) slider position error; (c) cable tension related to joint torque through (2); and (d) tip motion in the Cartesian space.

Fig. 9(a) and (b) reports joint positions and joint error in norm for the case of control law (3). Instead, Fig. 10(a) and (b) show joint positions and slider position error in norm in the case of control law (4). The cable tension generated by the two control laws and the Cartesian behavior in terms of index finger tip motion are finally reported in Figs. 9(c) and (d) and 10(c) and (d).

The error time evolution emphasizes the rapid convergence to zero, the small norm value and the good stability of the control in the slider space. Moreover, with respect to the control in the joint space, it reduces joint oscillations due to the springs at the joints [Figs. 9(b) and 10(b)]. Globally, simulation results show that the PD control in the slider space with elastic compensation

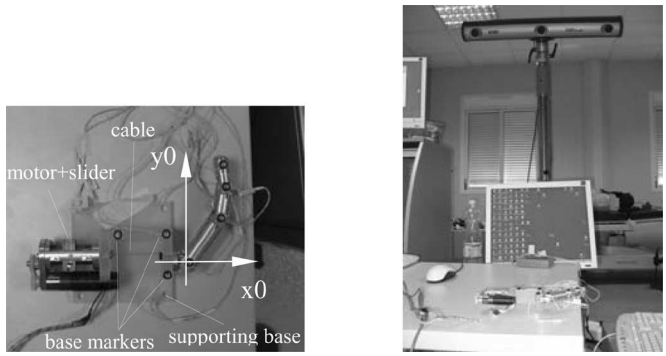

Fig. 11. Experimental setup: supporting base with the actuation system and the artificial finger on the left; and the OPTOTRAK Certus system on the right.

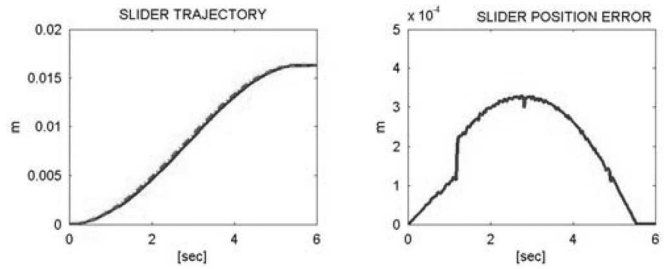

Fig. 12. Experimental results for the control in the slider space: (a) desired slider trajectory (dashed–dotted line) and actual trajectory (solid line); (b) slider position error.

seems to achieve better control performance with respect to the control in the joint space.

The control in the slider space has been also tested on the real artefact (Fig. 11) in order to validate the simulation model and the corresponding results. Basically, the experimental validation consists of implementing control law (4) through a FAULHABER electronic board, which allows providing the slider desired trajectory as control input to the dc motor. To this purpose, the same cubic polynomial trajectory as for the simulation tests has been used in input, and the slider position has been extracted in output by means of the encoder located on the motor. The experimental results about the control in the slider space are reported in Fig. 12.

The finger and the actuation system have been fixed to a supporting base. Due to the absence of sensors on the joints, joint trajectories have been recorded by means of the OPTOTRAK Certus system, which is an infrared optical device for movement analysis. In the future, hand prototype joint sensors will be embedded in the hand in order to obtain useful data during hand operation. Seven active infrared miniaturized markers have been placed on each finger joint and on the supporting base (Fig. 11) in order to refer the joint motion to a unique reference frame, as shown in Fig. 8.

The joint angles over time have been calculated from the acquired marker coordinates over time and the homogeneous transformation matrices, which allow moving from local coordinate systems to the base reference frame. The acquisition rate of the optical system is 30 Hz.

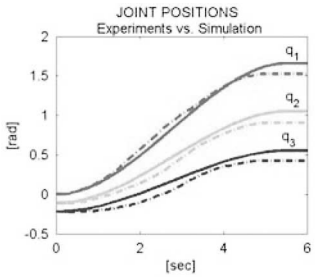

Fig. 13. Experimental results about joint positions. Solid lines are related to the measured joint positions while dashed–dotted lines are obtained by means of the simulation model.

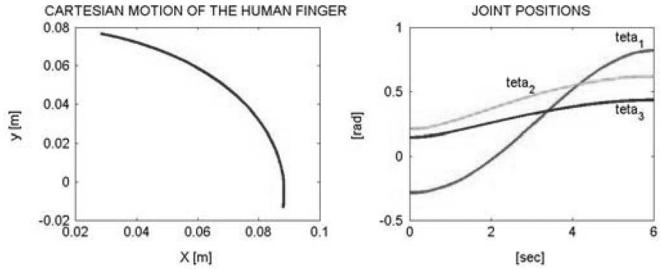

Fig. 14. (a) Tip motion in the Cartesian space for the human index finger. (b) Corresponding joint trajectories.

Fig. 13 shows the measured joint positions (dash-dot lines) overlapped to the finger joint positions extracted by the simulation model (solid lines). The experimental data in Figs. 12 and 13 appear to be very close to the model. The slight difference in the slider position error and between the joint curves is due to the friction between the cable and each pulley, which makes the tension reduce along the cable, while in the model the assumption is made that the tension is constant along the whole cable. As a consequence, the actuation torques decrease from the proximal to the distal joint causing a lower equilibrium joint angle.

B. Optimization Process of Mechanical and Control Design

In this section, the joint trajectories of the human finger and of the robotic finger are analyzed in order to address Goals 3 and 4, and complete the overall biomechatronic design process of the proposed robotic hand.

To this purpose, the authors have selected one specific motion task (i.e., preshaping for a palmar grasp of a cylindrical object, which is a basic key motor task enabling many activities of daily living) and reconstructed human motion by means of data extracted by the biomechanics literature. Studies on human motor control strategies [44] and trajectory generation during grasping tasks [15], [16] show that the tip trajectory that best fit the data recorded on the human index finger is the logarithmic spiral [15], [16]. In polar coordinates (r,θ) it can be expressed as

$$r = A\left(\exp\left(\theta\frac{\cos b}{\sin b}\right)\right)$$
$$A = 1.3394(l_d + l_m + l_p) - 23.255$$
$$b = 1.633 \tag{6}$$

where l_d, l_m, and l_p are the link lengths in the human case.

By reporting human data in the same reference frame used for the robotic finger and shown in Fig. 8, the index finger motion has been obtained in the Cartesian and joint space by means of the simulation software MATLAB/Simulink, under the assumption of index finger closing in a 2-D space in absence of gravity.

Thus, the logarithmic spiral reported in Cartesian coordinates can be described in terms of joint variables θ_1, θ_2, and θ_3 as

$$x = l_p\cos\theta_1 + l_m\cos(\theta_1+\theta_2) + l_d\cos(\theta_1+\theta_2+\theta_3)$$
$$y = l_p\sin\theta_1 + l_m\sin(\theta_1+\theta_2) + l_d\sin(\theta_1+\theta_2+\theta_3) \tag{7}$$

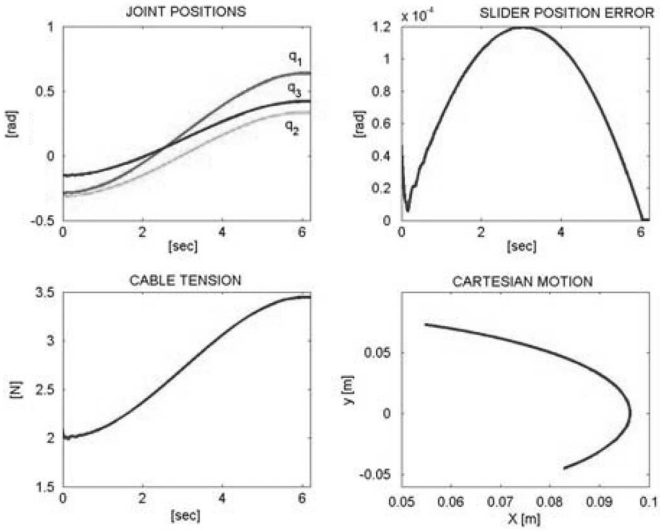

Fig. 15. Simulation results for the control in the slider space: (a) finger joint trajectories; (b) joint position error; (c) cable tension related to joint torque through (2); (d) tip motion in the Cartesian space.

where relation $\theta_3 = 0.7\theta_2$ seems to hold [15], [16]. From here, inverse kinematics allows extracting joint trajectories corresponding to the tip logarithmic spiral. In particular, condition $\theta_3 = 0.7\theta_2$ on the joints is used to solve redundancy in the plane. Simulation results are reported in Fig. 14.

The reconstructed motion of the human finger in the joint, as well as in the Cartesian space is now used to extract the reference signal for the control law (4), and compare motion of the robotic index finger with the human one. The reference slider motion for the robotic finger is obtained by replacing q_1, q_2, q_3 in (1) with human joint values θ_1, θ_2, and θ_3.

Simulation results in Fig. 15 show the joint positions, the norm error of the slider position, the cable tension, and the tip motion of the robotic finger when the dynamic model of the first finger prototype is used for the simulation tests. Thus, they are related to the same set of mechanical parameters reported in Section IV-A, i.e.,

- $K_e = \mathrm{diag}(10.93, 6.69, 5.03)10^{-3}$ N·m/rad;
- $r_1 = 7\times10^{-3}$ m, $r_2 = 3\times10^{-3}$ m, $r_3 = 2\times10^{-3}$ m;
- $q_0 = [-\pi/2 - 1.21 - 0.95]^T$;

and initial conditions

- $q_{i1} = -0.289$ rad (it is the initial position for the first finger joint, as in the human finger);
- $T_0 = 2$ N.

The control gains have been set to $K_{PS} = 2000$ and $K_{DS} = 100$.

At a glance, by observing joint positions and Cartesian motion in Figs. 14 and 15, it emerges that this set of mechanical parameters does not allow reproducing a human-like motion in hand closing, despite the stability of the control and the position error convergence to zero. In view of the coupling in the artificial hand dynamics and kinematics due to the cable-driven underactuation, the tip trajectory is quite far from the human trajectory, even if the time evolution of q_1 is very close to θ_1.

However, the integrated approach between mechanics and control offers the chance of putting together the potentials of CAD tools and control tools to parameterize the design of the artificial hand, and iteratively study the effect of progressive mechanical redesign on the motion behavior. The ultimate goal of this iterative approach is to minimize the error with respect to the motion of the human finger, and come to an 'optimal' set of mechanical and control parameters for the hand redesign.

In particular, the parametric model allows adjusting values of the preload q_0 that is the parameter mainly influencing the overall finger motion. On the other hand, spring stiffness coefficients play an important role in determining the final equilibrium configuration, while the radius values have a negligible effect on the finger motion. Instead, as outlined in Section II, r_1, r_2, and r_3 play a fundamental role in ensuring grasp stability.

Based on these considerations, the spring stiffness coefficients are chosen in order to satisfy the final static equilibrium of the human finger posture. Then, a set of reasonable preloads has been used in different simulations starting from the values that satisfy the initial static equilibrium of the human finger posture. From this analysis, the optimal set of mechanical parameters resulted in the following:

- $K_e = \mathrm{diag}(19.005, 21.898, 20.906)10^{-3}$ N·m/rad;
- $r_1 = 7 \times 10^{-3}$ m, $r_2 = 3 \times 10^{-3}$ m, $r_3 = 2 \times 10^{-3}$ m;
- $q_0 = [-1.391 - 0.204 - 0.142]^T$;

with initial conditions $q_{i1} = -0.289$ rad, $T_0 = 3$ N, and control gains $K_{PS} = 2000$ and $K_{DS} = 200$.

Note that the set of pulley radii are the same as of the first prototype obtained in previous studies of grasp stability.

In Fig. 16, the simulation results of the closed-loop optimized artificial system are reported, and in Fig. 17 the comparison with the human index finger is shown. Basically, the new set of mechanical parameters let the first joint follow the same trajectory as before (see Fig. 15), but visibly changes the behavior of joints q_2 and q_3. This entails a modification of the tip motion towards the target, i.e., the human logarithmic spiral in Cartesian coordinates, as desired.

Finally, simulation results have been verified in ADAMS, and three snapshots of the optimized finger performing the human-like motion are reported in Fig. 18.

So far, the validation of the proposed approach for optimization has been carried out through simulation tests. Experimental validation will be performed as soon as the new release of the hand prototype will be available.

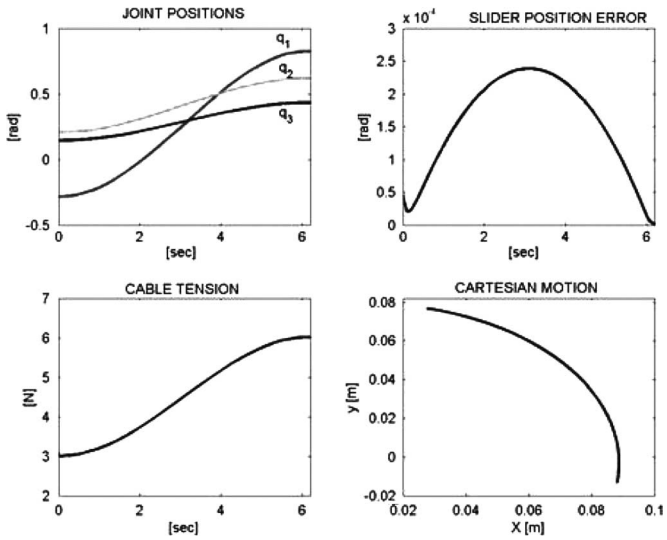

Fig. 16. Simulation results for the control in the slider space for a reference signal extracted by human data: (a) finger joint trajectories; (b) joint position error; (c) cable tension related to joint torque through (2); (d) tip motion in the Cartesian space.

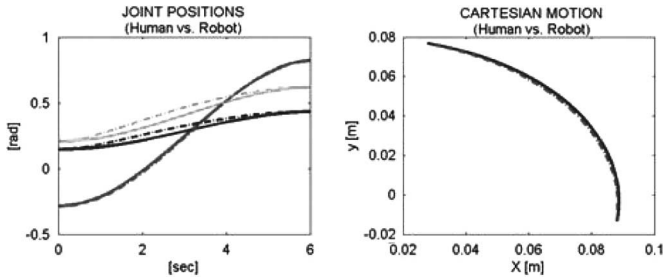

Fig. 17. Comparison between the artificial (solid line) and the human (dashed–dotted) index finger: (a) finger joint trajectories; (b) tip motion in the Cartesian space.

Fig. 18. Three ADAMS snapshots of the underactuated optimized finger showing the tip trajectory in three different time instants.

V. Conclusion

This paper presented a biomechatronic approach to the design of an anthropomorphic artificial hand, trying to address the requirements coming from two specific application fields, i.e., prosthetics and humanoid robotics.

The work specifically addressed the optimization of an existing artificial hand prototype by identifying the detailed refinements needed on the design of one finger in order to obtain an improved biomorphic behavior with respect to the natural hand.

Motivations and basic features of the initial mechanical design were reported in the first part of the paper. In particular, the concept of finger underactuation was explained, and the actuation system and the sensory system of each finger were described.

The mathematical formulation of the proposed control schemes focused on two simple PD control laws, which were significantly revisited to cope with the underactuation of the robotic hand. To this purpose, the problem was simplified to the control of a single underactuated finger. Simulation tests showed that only the PD control in the slider space is capable of properly controlling finger joints as desired, in terms of stability and biomorphic behavior. For the hand control, however, the approach has to be generalized to the control of multiple DOFs and completed with the study and control of multiple finger coordination.

The integrated approach to the design of mechanics and control led to the development of a parametric model of the artificial finger regarded as a closed-loop system. This model has been extensively used to iteratively optimize the design parameters of a single underactuated finger. In particular, the reliability of the developed parametric model, as well as of the control in the slider space have been experimentally validated on the first prototype of the artificial finger, which was designed for stable grasping tasks of a cylindrical object.

Finger optimization has been iteratively carried out on the parametric simulated model, and has led to define the set of optimal parameters that allow reproducing a human-like motion during preshaping. CAD tools have been used for a virtual reconstruction of the optimized finger motion.

Future experiments will be done with an optimal redesigned hand in order to validate the optimization process. This will include also a rerun of the process under different closing time next to the human ones. A sensitivity analysis will be performed in order to find the best set of optimization parameters. Additional work will address the extension of the proposed design approach to more complex tasks where fingers motion and dynamics are considered not only in the plane but in 3D space as well, and also the fingers coordination will be investigated. Some of the simplifying assumptions adopted so far (e.g., absence of gravitational effects, absence of friction between the cable and the pulley, presence of a sheath between the actuation system and each finger, etc.) will be removed. For instance, when different configurations of the arm holding the hand will be considered, the expression for $g(q)$ shall be generalized as a function of the joints of both the hand and the arm. This would be quite a challenging problem for prosthetic application. Moreover, the same simulation tools will be used to investigate the problem of multiple finger motor coordination during grasping and manipulation tasks, in order to pursue a human-like behavior for the control of the whole artificial hand.

ACKNOWLEDGMENT

The authors would like to thank Prof. B. Siciliano, R. Tucci, and L. Manfredi for their collaboration.

REFERENCES

[1] I. A. Kapandji, *The Physiology of the Joints: Upper Limb*, vol. 1, 5th ed. New York: Elsevier, 1986.

[2] R. M. Murray and S. S. Sastry, *A Mathematical Introduction to Robotic Manipulation*. Boca Raton, FL: CRC Press, 1993.

[3] A. Bicchi, "Hand for dexterous manipulation and robust grasping: A difficult road toward simplicity," *IEEE Trans. Robot. Autom.*, vol. 16, no. 6, pp. 652–662, Dec. 2000.

[4] W. T. Townsend, "The BarrettHand grasper—Programmably flexible part handling and assembling," *Ind. Robot*, vol. 27, pp. 181–188, 2000.

[5] J. Butterfass, M. Grebenstein, H. Liu, and G. Hirzinger, "DLR-hand II: Next generation of a dexterous robot hand," in *Proc. 2001 IEEE Int. Conf. Robot. Autom.*, Seoul, Korea, pp. 109–114.

[6] A. Ramos, I. A. Gravagne, and I. D. Walker, "Goldfinger: A non anthropomorphic, dexterous robot hand," in *Proc. 1999 IEEE Int. Conf. Robot. Autom.*, Detroit, MI, pp. 913–919.

[7] A. Eusebi, C. Fantuzzi, C. Melchiorri, M. Sandri, and A. Tondelli, "The UB hand II control system: Design features and experimental results," in *Proc. IEEE Int. Conf. Ind. Electron., Control Instrum.*, 1994, vol. 2, pp. 781–786.

[8] D. Reynaerts, "Control methods and actuation technology for whole-hand dexterous manipulation" Ph.D. dissertation, Prod. Eng. Mach. Design Autom., Catholic Univ. Leuven, Leuven, Belgium, 1995.

[9] Ottobock Orthopedic Industry GmbH, "MyoBock-arm components: 1997/98, Ottobock," in *Proc. 9th Annu. Conf. Magn. Jpn. Dig.*, 1982, p. 301.

[10] L. E. Rodriguez-Cheu and A. Casals, "Sensing and control of a prosthetic hand with myoelectric feedback," presented at the 1st IEEE/RAS-EMBS Int. Conf. Biomed. Robot. Biomechatron., Pisa, Italy, 2006.

[11] J. Zhao, Z. Xie, L. Jiang, H. Cai, H. Liu, and G. Hirzinger, "A five-fingered underactuated prosthetic hand control scheme," presented at the 1st IEEE/RAS-EMBS Int. Conf. Biomed. Robot. Biomechatron., Pisa, Italy, 2006.

[12] P. J. Kyberd, O. E. Holland, P. H. Chappel, S. Smith, R. Tregidgoi, and P. J. Bagwell, "MARCUS: A two degree of freedom hand prosthesis with hierarchical grip control," *IEEE Trans. Rehabil. Eng.*, vol. 3, no. 1, pp. 70–76, Mar. 1995.

[13] P. A. O'Neill *et al.*, "Myoelectric signal characteristics form muscles in residual upper limbs," *IEEE Trans. Rehabil. Eng.*, vol. 2, no. 4, pp. 266–270, Dec. 1994.

[14] L. Biagiotti, F. Lotti, C. Melchiorri, and G. Vassura, "An integrated approach to the design of complex robotic end-effectors," in *Proc. IEEE/ASME Int. Conf. Adv. Intell. Mechatron.*, Jul. 2003, vol. 1, pp. 70–75.

[15] D. G. Kamper, E. G. Cruz, and M. P. Siegel, "Stereotypical fingertip trajectories during grasp," *J. Neurophysiol.*, vol. 90, pp. 3702–3710, 2003.

[16] X. Luo, T. Kline, H. C. Fisher, K. A. Stubblefield, R. V. Kenyon, and D. G. Kamper, "Integration of augmented reality and assistive devices for post-stroke hand opening rehabilitation," presented at the Int. Conf. IEEE Eng. Med. Biol. Soc., Shanghai, China, 2005.

[17] P. Scherillo, B. Siciliano, L. Zollo, M. C. Carrozza, E. Guglielmelli, and P. Dario, "Parallel force/position control of a novel biomechatronic hand prosthesis," in *Proc. IEEE/ASME Int. Conf. Adv. Intell. Mechatron.*, Jul. 2003, vol. 2, pp. 920–925.

[18] M. R. Cutkosky, *Robotic Grasping and Fine Manipulation*. Boston, MA: Kluwer, 1985.

[19] I. D. Walker, A. Freeman, and S. I. Marcus, "Analysis of motion and internal loading of objects grasped by multiple cooperating manipulators," *Int. J. Robot. Res.*, vol. 10, pp. 396–407, 1991.

[20] J. L. Nevins and D. E. Whitney, "The force vector assembler concept," in *Proc. 1st CISM-IFToMM Symp. Theory Practice Robots Manipulators*, 1973.

[21] J. K. Salisbury, "Active stiffness control of a manipulator in Cartesian coordinates," in *Proc. IEEE Conf. Dec. Control*, 1980, vol. 1, pp. 95–100.

[22] J. Simons and H. Van Brussel, *Force Control Schemes for Robot Assembly*, K. Rathmill, Ed. Berlin, Germany: Robotic Assembly, 1985, pp. 253–265.

[23] L. Zollo, L. Dipietro, B. Siciliano, E. Guglielmelli, and P. Dario, "A bio-inspired approach for regulating and measuring visco-elastic properties of a robot arm," *J. Robot. Syst.*, vol. 22, pp. 397–419, 2005.

[24] L. Zollo, B. Siciliano, A. De Luca, E. Guglielmelli, and P. Dario, "Compliance control for an anthropomorphic robot with elastic joints: Theory and experiments," *Trans. ASME, J. Dyn. Syst., Meas. Control*, vol. 127, pp. 321–328, 2005.

[25] D. Formica, L. Zollo, and E. Guglielmelli, "Torque-dependent compliance control in the joint space for robot-mediated motor therapy," *Trans. ASME, J. Dyn. Syst. Meas. Control*, vol. 128, pp. 152–158, 2006.

[26] N. Hogan, "Impedance control: An approach to manipulation, Part I," *Trans. ASME, J. Dyn. Syst. Meas. Control*, vol. 107, pp. 1–27, Mar. 1985.

[27] N. Hogan, "Impedance control: An approach to manipulation, Part II," *Trans. ASME, J. Dyn. Syst. Meas. Control*, vol. 107, pp. 8–16, Mar. 1985.
[28] N. Hogan, "Impedance control: An approach to manipulation, Part III," *Trans. ASME, J. Dyn. Syst. Meas. Control*, vol. 107, pp. 17–24, Mar. 1985.
[29] H. Kazerooni *et al*., "Robust compliant motion for manipulators. Part 1: The fundamental concepts of compliant motion," *IEEE Trans. Robot. Autom*., vol. 2, no. RA-2, pp. 83–105, Jun. 1986.
[30] H. Kazerooni *et al*., "Robust compliant motion for manipulators. Part 2: Design method," *IEEE Trans. Robot. Autom*., vol. 2, no. RA-2, pp. 83–105, Jun. 1986.
[31] K. B. Shimoga and A. A. Goldenberg, "Grasp admittance center: A concept and its implications," in *Proc. IEEE Int. Conf. Robot. Autom*., Sacramento, CA, 1991, pp. 293–298.
[32] M. H. Raibert and J. J. Craig, "Hybrid position/force control of manipulators," *Tran. ASME, J. Dyn. Syst. Meas. Control*, vol. 103, pp. 126–133, 1981.
[33] B. Siciliano and L. Villani, *Robot Force Control*. Boston, MA: Kluwer, 1999.
[34] L. Zollo, B. Siciliano, C. Laschi, G. Teti, and P. Dario, "An experimental study on compliance control for a redundant personal robot arm," *Robot. Auton. Syst*., vol. 44, pp. 101–129, 2003.
[35] B. Massa, S. Roccella, M. C. Carrozza, and P. Dario, "Design and development of an underactuated prosthetic hand," in *Proc. 2002 IEEE Int. Conf. Robot. Autom*., Washington, DC, pp. 3374–3379.
[36] S. Hirose and Y. Umetani, "The development of soft gripper for the versatile robot hand," *Mech. Mach. Theory*, vol. 13, pp. 351–359, 1978.
[37] M. C. Carrozza, C. Suppo, F. Sebastiani, B. Massa, F. Vecchi, R. Lazzarini, M. R. Cutkosky, and P. Dario, "The spring hand: Development of a self adaptive prosthesis for restoring natural grasping," *Auton. Robots*, vol. 16, pp. 125–141, 2004.
[38] L. Sciavicco and B. Siciliano, *Modelling and Control of Robot Manipulators*, 2nd ed. London, U.K.: Springer-Verlag, 2000.
[39] M. Higashimori, M. Kaneko, A. Namiki, and M. Ishikawa, "Design of the 100G capturing robot based on dynamic preshaping," *Int. J. Robot. Res*., vol. 9, pp. 743–753, 2005.
[40] M. Higashimori, S. Nishio, and M. Kaneko, "Dynamic preshaping based optimum design for high speed capturing robots," in *Proc. IEEE/RSJ Int. Conf. Intell. Robots Syst*., 2005, pp. 913–918.
[41] H. Cheng, L. Obergefell, and A. Rizer, "Generator of body (GEBOD) manual," Armstrong Lab., WPAFB, Dayton, OH, Rep. AL/CF-TR-1994-0051, 1994.
[42] R. Cabas and C. Balauger, "Design and development of a light weight embodied robotic hand activated with only one actuators," in *Proc. IEEE/RSJ Int. Conf. Intell. Robots Syst*., 2005, pp. 741–746.
[43] I. W. Park, J. Y. Kim, J. Lee, and J. H. Oh, "Mechanical design of humanoid robot platform KHR-3 (KAIST humanoid robot-3: HUBO)," in *Proc. 5th IEEE-RAS Int. Conf. Humanoid Robots*, 2005, pp. 321–326.
[44] E. R. Kandel, J. H. SchWartz, and T. M. Jessell, *Principles of Neural Science*, 4th ed. New York: McGraw-Hill, 2000.
[45] H. K. Fathy, P. Y. Papalambros, A. G. Ulsov, and D. Hrovat, "Nested plant/controller optimization with application to combined passive/active automotive suspensions," in *Proc. Amer. Control Conf*., Jun. 2003, vol. 4, pp. 3375–3380.
[46] H. K. Fathy, J. A. Reyer, P. Y. Papalambros, and A. G. Ulsoy, "On the coupling between the plant and controller optimization problems," in *Proc. Amer. Control Conf*., Arlington, VA, Jun. 2001, vol. 3, pp. 1864–1869.

Loredana Zollo received the Laurea degree (*cum laude*) in electrical engineering from the University of Naples, Naples, Italy, in October 2000, and the Research Doctorate degree in bioengineering from the Scuola Superiore Sant'Anna, Pisa, Italy, in May 2004.

In April 2000, she joined the Advanced Robotics Technology and Systems Laboratory, Scuola Superiore Sant'Anna. She was a Visiting Student at the Laboratory of Neuroscience INSERM483, University Pierre et Marie Curie, Paris, France. In January 2004, she collaborated with the Campus Biomedico University, Rome, Italy, on educational and scientific activities and participated in the startup of the Biomedical Robotics and EMC Laboratory. Her research interests include rehabilitation robotics, assistive robotics, and neurorobotics, especially the kinematic and dynamic analysis of robot manipulators; the design and development of control schemes for robot manipulators with elastic joints and flexible links; the design and development of control schemes of interaction robotic machines for rehabilitation robotics, biological motor control and neurophysiological models of sensory-motor coordination; and the design and development of motor control schemes for bio-inspired robotic systems, multisensory integration and sensory–motor coordination of anthropomorphic robotic systems.

Stefano Roccella received the Laurea degree in aeronautical engineering from the University of Pisa, Pisa, Italy, in February 1999, and the Ph.D. degree in robotics from the University of Genova, Genova, Italy.

In 1999, he joined the Advanced Robotic Technology and System Laboratory, Scuola Superiore Sant'Anna, Pisa, as a Research Assistant. Currently, he is an Assistant Professor of biomedical robotics at Scuola Sant'Anna. His research interests include biomedical robotics, rehabilitation engineering, biomechatronics, and MEMS design and development.

Eugenio Guglielmelli received the Laurea degree in electronics engineering and the Ph.D. degree in robotics from the University of Pisa, Pisa, Italy, in 1991 and 1995, respectively.

He is currently an Associate Professor of bioengineering at Campus Biomedico University, Rome, Italy, where he is the Head of the Research Unit on biomedical robotics. From 2002 to 2004, he was the Head of the Advanced Robotics Technology and Systems Laboratory, Scuola Superiore Sant'Anna, Pisa, where he has been working in the field of biomedical robotics over the last 15 years. He is a Principal Investigator in several projects funded by the European Commission under the VI Framework programme in the field of biomedical engineering. He serves on the program committees and is a member of the organizing committees of several international conference proceedings. He serves on the Editorial Board of the *International Journal on Applied Bionics and Biomechanics*. He has been the Guest Co-Editor of the special issues on rehabilitation robotics of *Autonomous Robots* and on robotics platforms for neuroscience of the *International Journal of Advanced Robotics*. His research interests include novel theoretical and experimental approaches to human-centered robotics and to biomporphic control of mechatronic systems, and in their application to robot-mediated motor therapy, assistive robotics, and neurodevelopmental engineering.

Prof. Guglielmelli is a member of the IEEE Robotics and Automation Society and the IEEE Engineering in Medicine and Biology Society. He served as Secretary of the IEEE Robotics and Automation Society (RAS) during 2002–2003, and is currently a Co-Chair of the RAS Technical Committee on Rehabilitation Robotics.

M. Chiara Carrozza received the Laurea degree in physics from the University of Pisa, Pisa, Italy, and the Ph.D. degree in engineering from the Scuola Superiore Sant'Anna, Pisa, in 1990 and 1994, respectively.

Since 2001, she has been an Associate Professor of biomedical robotics at the Scuola Superiore Sant'Anna, where she is the Director of the Research Division and is also its Deputy Director. She is the Coordinator of the Advanced Robotics Technology and Systems Laboratory, Scuola Superiore Sant'Anna. She is the co-founder of two spin-offs of the Scuola Superiore Sant'Anna and is a member of their administrative boards. She is an elected member of the national board of the Italian Association of Biomedical Engineering (Gruppo

Nazionale di Bioinegegneria). She was a Visiting Professor at the Technical University of Vienna, Vienna, Austria. Her research interests include biomedical robotics (cybernetic and robotic artificial hands, upper limb exoskeletons), rehabilitation engineering (neurorehabilitation, domotic, and robotic aids for functional support and personal assistance), and biomedical microengineering (microsensors, tactile sensors). She is the author of several scientific papers and international patents.

Prof. Carrozza is a member of the IEEE Robotics and Automation Society and the IEEE Engineering in Medicine and Biology Society.

Paolo Dario received the Dr. Eng. degree in mechanical engineering from the University of Pisa, Pisa, Italy, in 1977.

He is a Full Professor of biomedical robotics at the Scuola Superiore Sant'Anna, Pisa, Italy. He is the Director of Polo Sant'Anna Valdera and of the Research Center in microengineering of the Scuola Superiore Sant'Anna. He was a Visiting Professor at the Ecole Polytechnique Federale de Lausanne, Switzerland, and at Waseda University, Tokyo, Japan. His research interests include biorobotics, biomedical engineering, biomechatronics, and microengineering. He is the editor of four books on the subject of robotics, and the author of more than 200 scientific papers.

Dr. Dario was the President of the IEEE Robotics and Automation Society from 2001 to 2002, during which time he also served as an Associate Editor of the IEEE TRANSACTIONS ON ROBOTICS AND AUTOMATION. He has also been the co-chair of the technical committees of biorobotics and roboethics conferences.